Table 2 Cox's proportional hazard models for overall survival according to NX-PVKA, conventional DCP, NX-PVKA-R, AFP, and AFP-L3

Tumor marker	Overall survival			
	Univarite analysis		Multivariate analysis	
	HR (95% CI)	*P* value	HR (95% CI)	*P* value
NX-PVKA (mAU/mL)	72.11 (19.14: 236.8)	< 0.0001	81.32 (15.68: 353.5)	< 0.0001
Conventional DCP (mAU/mL)	25.28 (2.571: 109.7)	0.0117	0.098 (0.004: 1.121)	0.0622
NX-PVKA-R	66.55 (6.745: 364.4)	0.0021	38.19 (2.173: 316.4)	0.0190
AFP (ng/mL)	20.28 (4.462: 64.38)	0.0007	10.11 (1.238: 54.60)	0.0334
AFP-L3 (%)	3.038 (1.134: 7.593)	0.0279	1.787 (0.563: 5.109)	0.3094

95% CI, 95% confidential interval; AFP, alpha-fetoprotein; AFP-L3, L3 fraction of *Lens culinaris* agglutinin-reactive species of AFP; DCP, des-gamma-carboxy prothrombin; HR, hazard ratio (per change in each tumor marker over entire range); NX-PVKA-R, conventional DCP divided by NX-PVKA.

The results of uni- and multivariate analyses by Cox's proportional hazard model are outlined in Table 2. Univariate analyses indicated that all tumor markers were significant predictors of overall survival. Multivariate analysis revealed NX-PVKA as the strongest independent prognostic marker for overall survival ($P < 0.0001$; hazard ratio [HR], 81.32). The HR for overall survival of NX-PVKA was larger than that of NX-PVKA-R ($P < 0.0190$; HR, 38.19). We therefore decided to examine associations between NX-PVKA and clinical features in patients with HCC.

In additional analyses, we compared overall survival between HCC patients with the following NX-PVKA levels: < 100 mAU/mL; ≥ 100 mAU/mL; < 400 mAU/mL, and finally ≥ 400 mAU/mL. Median survival in the group with < 100 mAU/mL NX-PVKA (2572 days) was significantly greater than that in the ≥ 100 mAU/mL and < 400 mAU/mL NX-PVKA groups (969 days; $P = 0.0041$) as well as in the ≥ 400 mAU/mL NX-PVKA group (392 days; $P < 0.0001$; Fig. 1a). Those analyzed data were still significant after Bonferroni correction. Survival did not differ significantly between ≥ 100 mAU/mL and < 400 mAU/mL NX-PVKA and the ≥ 400 mAU/mL NX-PVKA groups ($P = 0.0549$). In a simplified analysis, patients with a NX-PVKA level ≥ 100 mAU/mL showed significantly lower survival rates compared to patients with < 100 mAU/mL NX-PVKA (Fig. 1b; $P = 0.0001$).

We also grouped HCC patients according to Child-Pugh class A, B, or C (Fig. 1c,d). We verified the utility of NX-PVKA in predicting patient prognosis independent of hepatic functional reserve as determined by the Child-Pugh classification. Patients with a NX-PVKA level ≥ 100 mAU/mL displayed significantly lower survival rates than patients with < 100 mAU/mL NX-PVKA in both the Child-Pugh A ($P = 0.0002$) and Child-Pugh B or C subgroups ($P = 0.0026$).

To evaluate the influence of NX-PVKA levels on survival according to the TNM classification, we divided patients into two TNM subgroups: those with TNM stage I or II; and those with TNM stage III or IV (Fig. 1e,f). In both TNM subgroups, patients with higher NX-PVKA levels (≥ 100 mAU/mL) exhibited significantly lower survival rates ($P = 0.0275$ in the TNM stage I or II subgroup; $P = 0.0062$ in the TNM stage III or IV subgroup). Serum levels of NX-PVKA could thus offer a clinical prognostic factor in patients with advanced HCC.

Taken together, a ≥ 100 mAU/mL serum level of NX-PVKA could indicate poor prognosis among patients with HCC, independent of Child-Pugh or TNM classifications of cancer stage.

Tumor markers associated with clinical features and tumor factors. As illustrated in Supplemental Table S1, univariate regression analysis revealed that the following factors were significantly correlated with log NX-PVKA: bilirubin; albumin; aspartate aminotransferase; alanine aminotransferase (ALT); cholinesterase; lactate dehydrogenase, alkaline phosphatase (ALP); γ-glutamyl transpeptidase (γ-GTP); leucine aminopeptidase (LAP); C-reactive protein (CRP); total cholesterol; type IV collagen 7s; hyaluronic acid; hemoglobin; platelet count; maximum tumor size; number of tumors; and presence of portal venous invasion.

The correlation between NX-PVKA and conventional DCP was significant ($P < 0.0001$), but the correlation coefficient between conventional DCP and NX-PVKA was low ($r = 0.525$) (Fig. 2). Levels of NX-PVKA were 136 mAU/mL (19–47 883 mAU/mL) in conventional DCP-positive HCC patients, and 23 mAU/mL (17–43 mAU/mL) in conventional DCP-negative HCC patients.

Multivariate analysis was performed for each tumor marker (conventional DCP, NX-PVKA, NX-PVKA-R, AFP, and AFP-L3) using stepwise regression modeling with minimum AIC to choose the best models for each dependent variable (Supplemental Table S2). Among the factors identified in univariate analysis, sex ($P = 0.0256$), CRP ($P = 0.0105$), platelet count ($P = 0.0013$), international normalized ratio of prothrombin time (PT [international normalized ratio, INR]) ($P = 0.0065$), maximum tumor size ($P < 0.0001$), number of nodules ($P = 0.0002$), and portal venous invasion ($P = 0.0284$) were significant independent predictors of NX-PVKA. The log of NX-PVKA was significantly associated with the same factors as log conventional DCP but not log NX-PVKA-R. All tumor factors were independently associated with both log NX-PVKA and log conventional DCP. However, PT (INR) was associated with NX-PVKA ($P = 0.0065$) but not with conventional DCP ($P = 0.0545$). Furthermore, direct bilirubin was significantly associated with log NX-PVKA-R ($P = 0.0031$) but not with log NX-PVKA (not extracted).

On the other hand, ALT and type IV collagen 7S were associated with both log AFP and AFP-L3 but not with log conventional DCP or NX-PVKA (Supplemental Table S2). Both AFP and AFP-L3 were more closely related to inflammation and fibrosis due to hepatitis than NX-PVKA or conventional DCP were. All tumor factors were significantly associated with log NX-PVKA and log conventional DCP. However, only the number of tumors was associated with log AFP, while only maximum tumor size was associated with AFP-L3.

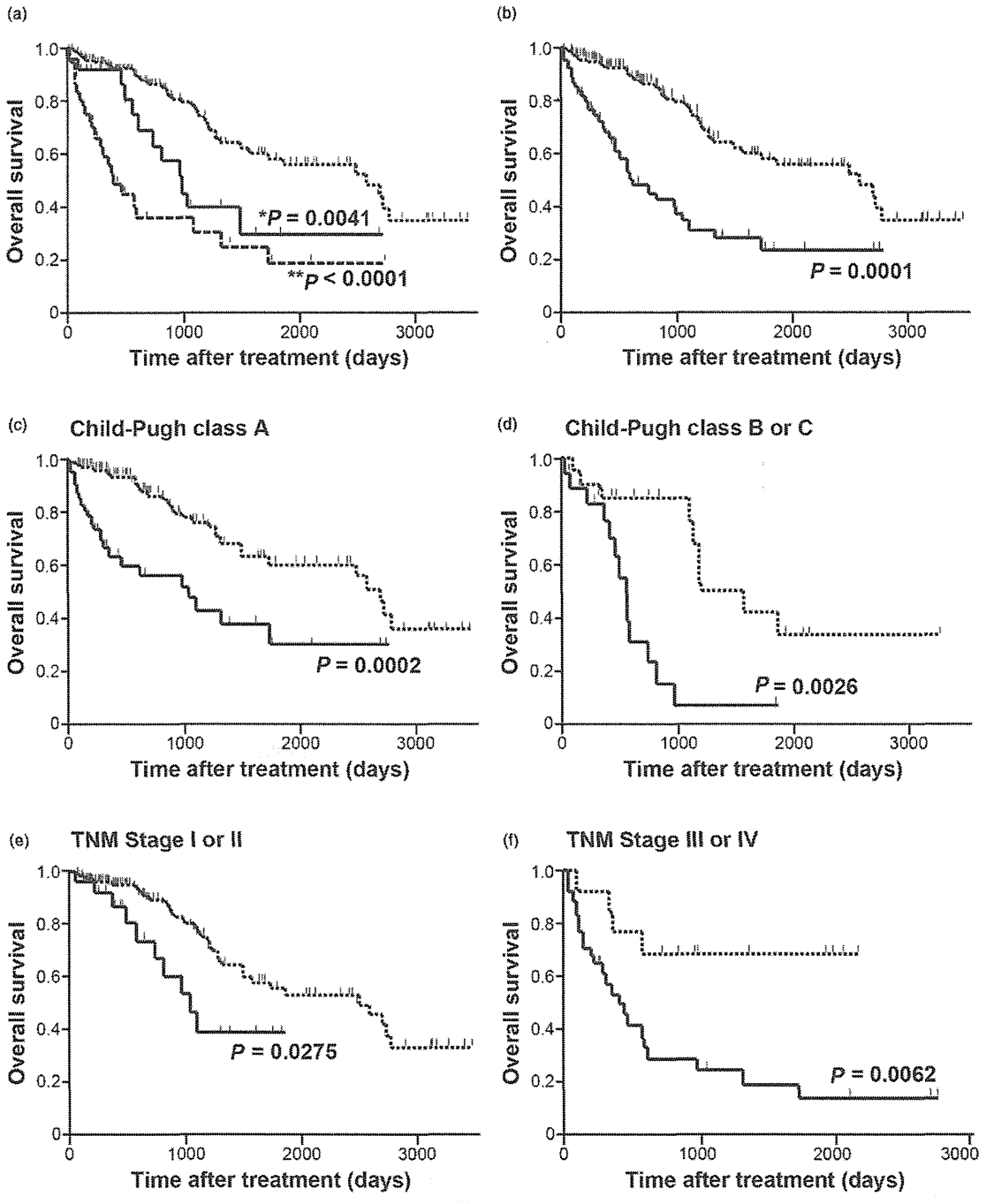

Figure 1 Overall survival of HCC patients with different levels of NX-PVKA. (a) Overall survivals of HCC patients with < 100 mAU/mL NX-PVKA, those with ≥ 100 mAU/mL and < 400 mAU/mL NX-PVKA, and those with ≥ 400 mAU/mL NX-PVKA. *Patients with 100–400 mAU/mL NX-PVKA showed significantly shorter survival than those with < 100 mAU/mL ($P = 0.0041$) and **those with ≥ 400 mAU/mL NX-PVKA ($P < 0.0001$). (b) When divided into only two groups, patients with ≥ 100 mAU/mL NX-PVKA showed significantly shorter survival than those with < 100 mAU/mL ($P = 0.0001$). This finding remained significant independent of Child-Pugh class A subgroup (c,d) and TNM stage (e,f). Kaplan-Meier survival analyses and log-rank testing were performed. Small vertical tick-marks in each figure indicate losses where patient survival was right-censored. ·····, NX-PVKA < 100; ——, 100 ≤ NX-PVKA < 400; - - - -, 400 ≤ NX-PVKA; ·····, NX-PVKA < 100; ——, NX-PVKA ≥ 100; ·····, NX-PVKA < 100; ——, NX-PVKA ≥ 100; ·····, NX-PVKA < 100; ——, NX-PVKA ≥ 100; ·····, NX-PVKA < 100; ——, NX-PVKA ≥ 100; ·····, NX-PVKA < 100; ——, NX-PVKA ≥ 100.

Table 3 Multivariate analysis by Cox's proportional hazard model for overall survival according to statistically significant prognostic factors

	HR	(95% CI)	RC	(95% CI)	*P* value
Gender [Male/Female]	3.70	(1.74: 8.86)	6.54×10^{-1}	(2.76×10^{-1}: 10.9×10^{-1})	0.0004
Albumin (g/dL)	5.11×10^{-2}	(0.85×10^{-2}: 33.9×10^{-2})	-8.04×10^{-1}	(-12.9×10^{-1}: -2.92×10^{-1})	0.0024
γ-GTP (U/L)	2.88×10	(0.32×10: 23.7×10)	4.30×10^{-3}	(1.48×10^{-3}: 7.00×10^{-3})	0.0034
LAP (U/L)	1.94×10^{-2}	(0.05×10^{-2}: 36.7×10^{-2})	-1.02×10^{-2}	(-1.97×10^{-2}: -0.26×10^{-2})	0.0071
CRP (mg/dL)	4.30×10	(0.54×10: 20.4×10)	3.17×10^{-1}	(1.42×10^{-1}: 4.48×10^{-1})	0.0017
Hyaluronic acid (ng/mL)	6.84×10	(1.06×10: 35.6×10)	1.35×10^{-3}	(7.57×10^{-4}: 1.88×10^{-3})	< 0.0001
Log NX-PVKA (mAU/mL)	1.96×10	(0.66×10: 5.65×10)	8.68×10^{-1}	(5.52×10^{-1}: 11.8×10^{-1})	< 0.0001

The risk of mortality from hepatocellular carcinoma score (ROM score) calculated by using the prognostic model results of this analysis as below. ROM score = 0.654 × (1: male, 0: female) − 0.804 × Albumin + 0.0043 × γ-GTP − 0.0102 × LAP + 0.317 × CRP + 0.00135 × Hyaluronic acid + 0.868 × Log NX-PVKA

95% CI: 95% confidential interval; CRP, C-reactive protein; DCP, des-gamma-carboxy prothrombin; HR, hazard ratio (per change in each factor over entire range); LAP, leucine aminopeptidase; PT (INR): international normalized ratio of prothrombin time; RC, risk coefficient; WB, white blood cell; γ-GTP, γ-glutamyl transpeptidase.

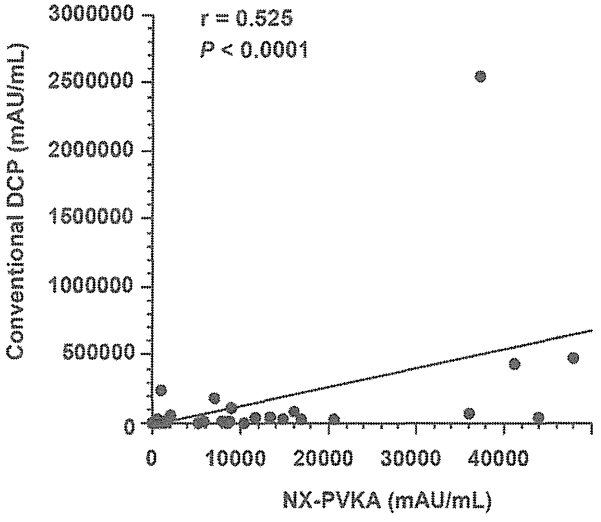

Figure 2 Correlation between NX-PVKA and conventional DCP. The correlation between NX-PVKA and conventional DCP is significant ($P < 0.0001$), although the correlation coefficient between conventional DCP and NX-PVKA is low (r = 0.525).

Results of uni- and multivariate analyses for overall survival by Cox's proportional hazard model are presented in Supplemental Table S3. Briefly, many clinical factors showed significant univariate associations with overall survival. For instance, all tumor markers, including log NX-PVKA, were significantly associated with overall survival. In addition, all three tumor factors listed in Supplemental Table S3 were significantly associated with overall survival. We excluded tumor factors from multivariate analysis and analyzed only the clinical factors listed in Supplemental Table S3. According to this analysis, log NX-PVKA was the only tumor factor that independently predicted overall survival ($P < 0.0001$). Other independent predictors of overall survival included sex ($P = 0.0001$), LAP ($P = 0.0072$), CRP ($P = 0.0094$), and hyaluronic acid ($P < 0.0001$).

Next, we sought to establish a prognostic model to estimate overall survival of patients using serum levels of log NX-PVKA. For this purpose, we used a stepwise regression model with the minimum AIC. The values identified in analyses are indicated in Table 3. The log of NX-PVKA, sex, albumin, γ-GTP, LAP, CRP, and hyaluronic acid were significant independent predictors of overall survival. From these results, we established a prognostic model for predicting overall survival in patients with HCC, which we named as the risk of mortality from HCC (ROM) score.

ROM score was calculated as follows: 0.654 × (1: male, 0: female) − 0.804 × Albumin + 0.0043 × γ-GTP − 0.0102 × LAP + 0.317 × CRP + 0.00135 × hyaluronic acid + 0.868 × log NX-PVKA

A higher ROM score indicates a lower duration of overall survival. Harrell's c-index is defined as the proportion of all usable patient pairs in which the predictions and outcome are concordant.[20] The index of correlation between ROM score and actual overall survival was 0.816.

We performed additional analyses to reveal the correlation between ROM score and overall survival of enrolled patients with HCC (Fig. 3), revealing a significant correlation (r = 0.644, $P < 0.0001$). Based on the results (Fig. 3), survival from the initiation of HCC treatment could be estimated using the following formula:

$$\log(\text{survival [days]}) = 6.311 - 0.529 \times \text{ROM score}.$$

Discussion

The present study identified serum levels of NX-PVKA, as the new variants of DCP, as the most significant prognostic tumor marker for HCC. Using NX-PVKA, we established a prognostic model that can estimate the duration of overall survival of HCC patients using clinical data.

NX-PVKA could be considered to overlap with DCP, which is produced by vitamin K deficiency.[7] With the exception of patients taking warfarin, NX-PVKA was the most effective prognostic marker among HCC patients. The clinical features associated with NX-PVKA were similar to those associated with conventional DCP but differed from those associated with AFP and AFP-L3 (Table 3). Both NX-PVKA and conventional DCP were closely related to tumor factors and platelet count, whereas AFP and AFP-L3 were not. AFP-L3 was found to be a useful

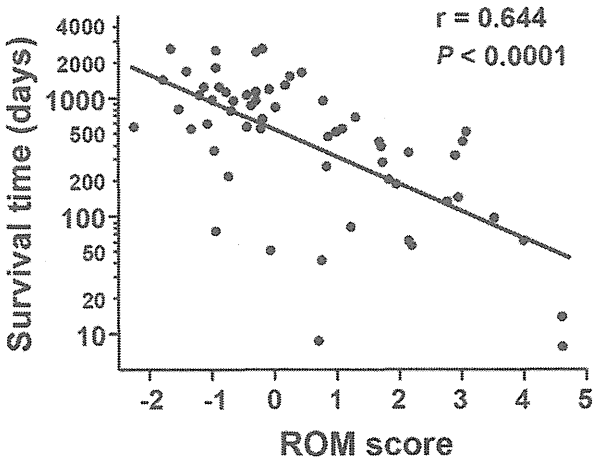

Figure 3 Correlation between risk of mortality (ROM) score from hepatocellular carcinoma (HCC) and patient. ROM score was calculated according to the following formula:
ROM score = 0.654 × (1: male, 0: female) − 0.804 × albumin + 0.0043 × γ-GTP − 0.0102 × LAP + 0.317 × CRP + 0.00135 × hyaluronic acid + 0.868 × log NX-PVKA.
ROM score correlated significantly with patient survival ($r = 0.644$, $P < 0.0001$). From this analysis, survival of each patient was estimated using the following equation:
log (survival [days]) = 6.311 − 0.529 × ROM score.

prognostic marker when serum concentrations of AFP were very low.[21,22] However, other reports suggest that DCP was superior to AFP in predicting disease prognosis.[23,24] Our data show general agreement with these previous reports. In addition, only NX-PVKA was associated with PT (INR). Based on univariate analysis, higher direct bilirubin correlated with high serum levels of NX-PVKA but not conventional DCP. NX-PVKA was more closely associated with hepatic functional reserve than conventional DCP was.

The expression of DCP occurs in HCC tissue, as well as in the surrounding non-HCC tissue. Inagaki *et al.* reported that the expression of DCP in both HCC and non-HCC tissues, and serum levels of DCP, were significantly related to postoperative survival in patients with HCC and liver cirrhosis.[19] Expression of DCP variants with less than 6 Glu residues was relatively higher among patients with nonmalignant liver diseases such as chronic hepatitis and liver cirrhosis than among those with HCC.[25] Hence, NX-PVKA, which comprises DCP with around 5 Glu residues, might be produced by chronically damaged liver tissue surrounding the HCC. Since HCC patients usually suffer from chronic liver injury, these notions may explain why NX-PVKA levels reflect hepatic functional reserve and best predict disease prognosis among HCC patients.

The structure of DCP contains two kringle domains similar to those of hepatocyte growth factor (HGF).[26] Moreover, DCP is thought to induce proliferation of HCC cells through HGF-like functions.[27] One reason why NX-PVKA and conventional DCP could be associated with tumor factors could be explained by the functional similarity to HGF. Direct effects of NX-PVKA on HCC tumor factors should be examined in future studies.

Multivariate analyses revealed that platelet count was positively associated with levels of both conventional DCP and NX-PVKA (Table 3). Poor hepatic functional reserve is well known to be related to decreased platelet counts in chronic liver injury.[28,29] From this perspective, the positive correlations between platelet count and both NX-PVKA and conventional DCP cannot be explained by the status of hepatic functional reserve. Others have reported that platelet count correlates with serum vascular endothelial growth factor levels in cancer patients, including those with HCC.[30] Moreover, platelet count is reportedly elevated in HCC patients with portal venous invasion[14] or extrahepatic metastasis.[18] Higher serum levels of NX-PVKA and conventional DCP with a higher platelet count would reflect tumor growth and portal venous invasion, which would contribute to the prognosis of HCC patients.

Several prognostic scoring systems have been proposed for HCC patients, including the CLIP score,[31] BCLC score,[32] and Tokyo score.[33] However, these scoring systems included tumor factors that had to be evaluated by diagnostic imaging. The present study proposed a prognostic model using only patient demographics and laboratory data. The proposed prognostic model could be useful for clinicians who do not regularly perform diagnostic imaging, or in outpatient clinics, when clinicians need to estimate approximate durations of overall survival for HCC patients. Moreover, the HCC stage could also be classified using these indices.

Several limitations must be considered when interpreting the present findings. First, this was a retrospective study of patients from a single center in Japan. Validation of the prognostic model in a prospective study is required. Second, HCC patients enrolled in this study had several etiologies of liver damage and received different treatments. Although the value of NX-PVKA was not influenced by the etiology of liver damage or treatment type, we need to perform similar experiments with a greater number of patients in each subgroup.

In conclusion, serum levels of NX-PVKA offered the most significant tumor marker predictor of prognosis among HCC patients in this study. The proposed prognostic model could be useful in estimating overall survival for HCC patients. We expect to conduct a prospective study of these findings in the near future.

Acknowledgments

The authors are grateful to Drs Jun Nishimura and Masao Uehara (EIDIA, Tokyo Japan) for their support in measuring NX-PVKA, and to Ms Satomi Nakayama, Ms Takana Fujino, and Ms Sakiko Inoh for their valuable technical assistance. This work was supported in part by a Grant-in-Aid for Scientific Research (JSPS KAKENHI 24590980 to Y.H.) and the Program for Enhancing Systematic Education in Graduate School (to S.T.) from the Japanese Ministry of Education, Culture, Sports, Science and Technology, as well as a Grant-in-Aid for Scientific Research and Development from the Japanese Ministry of Health, Labor and Welfare to Y.H.

References

1 El-Serag HM, Lenhard RK. Hepatocellular carcinoma: epidemiology and molecular carcinogenesis. *Gastroenterology* 2007; **132**: 2557–76.

2 Blanchard RA, Furie BC, Kruger SF, Waneck G, Jorgensen MJ, Furie B. Immunoassays of human prothrombin species which correlate with functional coagulation activities. *J. Lab. Clin. Med.* 1983; **101**: 242–55.
3 Liebman HA, Furie BC, Tong MJ *et al.* Des-gamma-carboxy (abnormal) prothrombin as a serum marker of primary hepatocellular carcinoma. *N. Engl. J. Med.* 1984; **310**: 1427–31.
4 Okuda H, Nakanishi T, Takatsu K *et al.* Measurement of serum levels of des-gamma-carboxy prothrombin in patients with hepatocellular carcinoma by a revised enzyme immunoassay kit with increased sensitivity. *Cancer* 1999; **85**: 812–18.
5 Bajaj SP, Price PA, Russell WA. Decarboxylation of gamma-carboxyglutamic acid residues in human prothrombin. *J. Biol. Chem.* 1982; **257**: 3726–31.
6 Naraki T, Kohno N, Saito H *et al.* γ-Carboxyglutamic acid content of hepatocellular carcinoma-associated des-γ-carboxy prothrombin. *Biochim. Biophys. Acta* 2002; **1586**: 287–98.
7 Toyoda H, Kumda T, Osaki Y *et al.* Novel method to measure serum levels of des-gamma-carboxy prothrombin for hepatocellular carcinoma in patients taking warfarin: a preliminary report. *Cancer Sci.* 2012; **103**: 921–5.
8 Aoyagi Y, Isemura M, Suzuki Y *et al.* Fucosylated alpha-fetoprotein as marker of early hepatocellular carcinoma. *Lancet* 1985; **326**: 1353–4.
9 Sato Y, Nakata K, Kato Y *et al.* Early recognition of hepatocellular carcinoma based on altered profiles of alpha-fetoprotein. *N. Engl. J. Med.* 1993; **328**: 1802–6.
10 Motohara K, Endo F, Matsuda I. Effect of vitamin K administration on acarboxyprothrombin (PIVKA-II) levels in newborns. *Lancet* 1985; **326**: 242–4.
11 Motohara K, Kuroki Y, Kan HK *et al.* Detection of vitamin deficiency by use of an enzyme-linked immunosorbent assay for circulating for circulating abnormal prothrombin. *Pediatr. Res.* 1985; **19**: 354–7.
12 Akaike H. A new look at statistical model identification. *IEEE Trans. Automat. Control* 1974; **19**: 716–23.
13 Suehiro T, Sugimachi K, Matsumata T, Itasaka H, Taketomi A, Maeda T. Protein induced by vitamin K absence or antagonist II as a prognostic marker in hepatocellular carcinoma. *Cancer* 1994; **73**: 2464–9.
14 Hagiwara S, Kudo M, Kawasaki T *et al.* Prognostic factors for portal venous invasion in patients with hepatocellular carcinoma. *J. Gastroenterol.* 2006; **41**: 1214–9.
15 Hakamada K, Kimura N, Miura T *et al.* Des-gamma-carboxy prothrombin as an important prognostic indicator in patients with small hepatocellular carcinoma. *World J. Gastroenterol.* 2008; **14**: 1370–7.
16 Kobayashi M, Ikeda K, Kawamura Y *et al.* High serum des-gamma-carboxy prothrombin level predicts poor prognosis after radiofrequency ablation of hepatocellular carcinoma. *Cancer* 2009; **115**: 571–80.
17 Yamashita Y, Tsuijita E, Takeishi K *et al.* Predictors for microinvasion of small hepatocellular carcinoma < 2 cm. *Ann. Surg. Oncol.* 2012; **19**: 2027–34.
18 Bae HM, Lee JH, Yoon JH, Kim YJ, Heo DS, Lee HS. Protein induced by vitamin K absence or antagonist-II production is a strong predictive marker for extrahepatic metastases in early hepatocellular carcinoma: a prospective evaluation. *BMC Cancer* 2011; **11**: 435–45.
19 Inagaki Y, Xu HL, Hasegawa K *et al.* Des-gamma-carboxyprothrombin in patients with hepatocellular carcinoma and liver cirrhosis. *J. Dig. Dis.* 2011; **12**: 481–8.
20 Harrell FE Jr, Lee KL, Califf RM *et al.* Regression modeling strategies for improved prognostic prediction. *Stat. Med.* 1984; **3**: 143–52.
21 Kobayashi M, Kuroiwa T, Suda T *et al.* Fucosylated fraction of alpha-fetoprotein, L3, as a useful prognostic factor in patients with hepatocellular carcinoma with special reference to low concentrations of serum alpha-fetoprotein. *Hepatol. Res.* 2007; **37**: 914–22.
22 Nouso K, Kobayashi Y, Nakamura S *et al.* Prognostic importance of fucosylated alpha-fetoprotein in hepatocellular carcinoma patients with low alpha-fetoprotein. *J. Gastroenterol. Hepatol.* 2011; **26**: 1195–200.
23 Inagaki Y, Tang W, Makuuchi M, Hasegawa K, Sugawara Y, Kokudo N. Clinical and molecular instates into the hepatocellular carcinoma tumour marker des-γ-carboxy prothrombin. *Liver Int.* 2011; **31**: 22–35.
24 Tang W, Miki K, Kokudo N *et al.* Des-gamma-carboxy prothrombin in cancer and non-cancer liver tissue of patients with hepatocellular carcinoma. *Int. J. Oncol.* 2003; **22**: 969–75.
25 Uehara S, Gotoh K, Handa H *et al.* Distribution of the heterogeneity of des-γ-carboxyprothrombin in patients with hepatocellular carcinoma. *J. Gastroenterol. Hepatol.* 2005; **20**: 1545–52.
26 Nakamura T, Nishizawa T, Hagiya M *et al.* Molecular cloning and expression of human hepatocyte growth factor. *Nature* 1989; **342**: 440–3.
27 Suzuki M, Shiraha H, Fujikawa T *et al.* Des-gamma-carboxy prothrombin is a potential autologous growth factor for hepatocellular carcinoma. *J. Biol. Chem.* 2005; **280**: 6409–15.
28 Pohl A, Behling C, Oliver D *et al.* Serum aminotransferase levels and platelet counts as predictors of degree of fibrosis in chronic hepatitis C virus infection. *Am. J. Gastroenterol.* 2001; **96**: 3142–6.
29 Shah AG, Lydecker A, Murray K *et al.* Comparison of noninvasive markers of fibrosis in patients with nonalcoholic fatty liver disease. *Clin. Gastroenterol. Hepatol.* 2009; **7**: 1104–12.
30 Koike Y, Shiratori Y, Sato S *et al.* Des-gamma-carboxy prothrombin as a useful predisposing factor for the development of portal venous invasion in patients with hepatocellular carcinoma. *Cancer* 2001; **91**: 561–9.
31 The Cancer of the Liver Italian Program (CLIP) Investigators. A new prognostic system for hepatocellular carcinoma: a retrospective study of 435 patients. *Hepatology* 1998; **28**: 751–5.
32 Llovet JM, Bru C, Bruix J. Prognosis of hepatocellular carcinoma: the BCLC staging classification. *Semin. Liver Dis.* 1999; **19**: 329–38.
33 Tateishi R, Yoshiba H, Shiina S *et al.* Proposal of a new prognostic model for hepatocellular carcinoma: an analysis of 403 patients. *Gut* 2005; **54**: 419–25.

Supporting information

Additional Supporting Information may be found in the online version of this article at the publisher's web-site:

Table S1 Univariate associations between various clinical and tumor factors and Log NX-PVKA, Log conventional DCP, Log NX-PVKA-R, Log AFP and AFP-L3.

Table S2 Multivariate stepwise regression analysis between various clinical and tumor factors and Log NX-PVKA, Log conventional DCP, Log NX-PVKA-R, Log AFP and AFP-L3.

Table S3 Cox's proportional hazard model for overall survival according to clinical and tumor factors.

Appendix S1 The method of NX-PVKA measurement.

OPEN ACCESS Freely available online

PLOS ONE

Protein Kinase R Modulates c-Fos and c-Jun Signaling to Promote Proliferation of Hepatocellular Carcinoma with Hepatitis C Virus Infection

Takao Watanabe[1], Yoichi Hiasa[1]*, Yoshio Tokumoto[1], Masashi Hirooka[1], Masanori Abe[1], Yoshio Ikeda[1], Bunzo Matsuura[1], Raymond T. Chung[2], Morikazu Onji[1]

1 Department of Gastroenterology and Metabology, Ehime University Graduate School of Medicine, Toon, Ehime, Japan, **2** Gastrointestinal Unit, Massachusetts General Hospital and Harvard Medical School, Boston, Massachusetts, United States of America

Abstract

Double-stranded RNA-activated protein kinase R (PKR) is known to be upregulated by hepatitis C virus (HCV) and overexpressed in hepatocellular carcinoma (HCC). However, the precise roles of PKR in HCC with HCV infection remain unclear. Two HCV replicating cell lines (JFH-1 and H77s), generated by transfection of Huh7.5.1 cells, were used for experiments reported here. PKR expression was modulated with siRNA and a PKR expression plasmid, and cancer-related genes were assessed by real-time PCR and Western blotting; cell lines were further analyzed using a proliferation assay. Modulation of genes by PKR was also assessed in 34 human HCC specimens. Parallel changes in c-Fos and c-Jun gene expression with PKR were observed. Levels of phosphorylated c-Fos and c-Jun were upregulated by an increase of PKR, and were related to levels of phosphorylated JNK1 and Erk1/2. DNA binding activities of c-Fos and c-Jun also correlated with PKR expression, and cell proliferation was dependent on PKR-modulated c-Fos and c-Jun expression. Coordinate expression of c-Jun and PKR was confirmed in human HCC specimens with HCV infection. PKR upregulated c-Fos and c-Jun activities through activation of Erk1/2 and JNK1, respectively. These modulations resulted in HCC cell proliferation with HCV infection. These findings suggest that PKR-related proliferation pathways could be an attractive therapeutic target.

Citation: Watanabe T, Hiasa Y, Tokumoto Y, Hirooka M, Abe M, et al. (2013) Protein Kinase R Modulates c-Fos and c-Jun Signaling to Promote Proliferation of Hepatocellular Carcinoma with Hepatitis C Virus Infection. PLoS ONE 8(7): e67750. doi:10.1371/journal.pone.0067750

Editor: Erica Villa, University of Modena & Reggio Emilia, Italy

Received February 25, 2013; **Accepted** May 22, 2013; **Published** July 2, 2013

Funding: This work was supported in part by the following: a Grant-in-Aid for Scientific Research, Japan Society for the Promotion of Science, KAKENHI 24590980 (to Y.H.); the Program for Enhancing Systematic Education in Graduate School from the Ministry of Education, Culture, Sports, Science and Technology, Japan (to T.W.); and by a Grant-in-Aid for Scientific Research and Development from the Japanese Ministry of Health, Labor and Welfare, Japan (to Y.H.). The funders had no role in study design, data collection and analysis, decision to publish, or preparation of the manuscript.

Competing Interests: The authors have declared that no competing interests exist.

* E-mail: hiasa@m.ehime-u.ac.jp

Introduction

Hepatitis C virus (HCV) is a leading cause of chronic liver disease and is a leading indication for liver transplantation [1]. HCV establishes persistent infection and induces chronic hepatitis, which leads to liver cirrhosis (LC) and, frequently, to hepatocellular carcinoma (HCC) [2]. However, the precise mechanisms involved in the induction of heptocarcinogenesis by HCV, and details of viral effects on tumor progression, remain unclear.

Of the many cellular proteins stimulated by HVC replication, double-stranded RNA-activated protein kinase R (PKR) appears to play a key antiviral role [3]. Double stranded-RNA produced by RNA viral replication is known to be a potent activator of PKR [4]. Activated PKR, in turn, induces PKR phosphorylation, and then PKR dimerizes and phosphorylates eukaryotic initiation factor-2 alpha (eIF2α), which inhibits protein synthesis, including that of virally-encoded proteins [5]. Moreover, PKR is recognized as a key arm of the antivirus and antiproliferative effects of interferon, the most important clinically active agent against HCV [3]. PKR plays multiple roles in cell growth, differentiation, apoptosis, and responses to cellular stress occurring during RNA virus infections [6].

The HCV generates dsRNA during the process of viral replication, which is thought to activate PKR and then induce the host antiviral responses [7]. Several reports have indicated that PKR can directly inhibit HCV replication [7–9]. We previously reported that PKR was overexpressed and activated in HCC with HCV infection, as compared with surrounding non-HCC tissues [10]. Moreover, the level of HCV-RNA was detected and reduced in HCC compared with surrounding non-HCC tissue, indicating that the overexpressed PKR in HCC tissues retains its antiviral function against HCV [10].

PKR was originally thought to function as a tumor suppressor protein, as it induces the apoptotic response [11,12], and it was suggested that PKR inhibits cell growth and proliferation [13,14]. However, results of further studies demonstrating functioning PKR in HCC with HCV infection [10] suggest that it could act as a tumor stimulator rather than as a suppressor.

The aim of this study was to identify the roles of PKR in HCC with HCV infection, and to evaluate whether overexpressed PKR in HCC has beneficial or malignant effects in patients with this disease.

Materials and Methods

Cell Culture and Transfection

The hepatoma cell line Huh 7.5.1 (kindly provided by Dr. Francis V. Chisari, Department of Immunology and Microbial Science, The Scripps Research Institute, La Jolla, CA, USA) was grown and maintained in Dulbecco's modified Eagle's medium (DMEM) (Life Technologies, Carlsbad, CA, USA) supplemented with 10% fetal bovine serum (FBS) (Life Technologies) and 1% penicillin. Cells were maintained at 37°C in a humidified atmosphere of 5% CO_2 and 95% air, and the culture medium was changed three times per week.

HCV-infected HCC cell lines used were JFH1 and H77s. JFH1 cells were generated by transfection of Huh 7.5.1cells with HCV-RNA synthesized by transcription from pJFH1-full (kindly provided by Dr. Takaji Wakita, National Institute of Infectious Diseases, Tokyo, Japan), which encodes the HCV genotype 2a sequence [15]. For the HCV-RNA transfection, Huh 7.5.1 cells were resuspended in Opti-MEM I (Life Technologies) containing 10 μg of synthesized HCV-RNA, and were subjected to an electric pulse (960 μF, 260 V) using the Gene Pulser II apparatus (Bio-Rad, Richmond, CA, USA). H77s cells were made by transfection with HCV-RNA transcripted from pH77s-full (kindly provided by Dr. Stanley M. Lemon, University of North Carolina at Chapel Hill, Chapel Hill, NC, USA), which encodes the HCV genotype 1a sequence [16,17]; the transfection procedure was the same as that previously described.

Patients and Liver Specimens

HCC specimens were obtained from patients who underwent surgery at our institution from 2007 to 2012. Written informed consent was obtained from all patients. The study protocol conformed to the ethical guidelines of the Declaration of Helsinki, and was approved by the Institutional Review Board at Ehime University Hospital (Approval No. 0710004). This study was registered by the University Hospital Medical Information Network (UMIN) Clinical Trials Registry (registration number 000008652). Table 1 lists clinicopathological features of the 34 HCC patients enrolled. Among the 34 specimens, 17 were from patients with HCV.

Samples of freshly resected liver specimens were incubated with RNAlater (Life Technologies) overnight at 4°C, and were then frozen and stored at −80°C until used. Additional samples were placed on dry ice and frozen immediately, and then stored at −80°C until used for protein extraction.

RNA Interference and PKR Inhibitor Assay

A PKR-specific siRNA (GAG AAU UUC CAG AAG GUG A, nt. 584–604) was designed using a PKR sequence template (accession number NM002759), and was then synthesized by Thermo Fisher Scientific (Waltham, MA, USA) [18]. Control siRNA was obtained from Cosmo Bio (Tokyo, Japan); c-Fos siRNA and c-Jun si-RNA were obtained from Thermo Fisher Scientific. Huh 7.5.1, JFH1 and H77s cell lines at 50% confluence in 6-well plates were transfected with 50 pM siRNA using RNAiMax (Life Technologies). For the assay with a PKR inhibitor, JFH1 or H77s cells were incubated with 300 nM of PKR inhibitor (Merck, Darmstadt, Deutschland) for 24 h.

PKR Plasmids

Plasmids encoding PKR genes were kindly provided by Dr. Michael Gale, Jr. (University of Washington, Seattle, WA, USA) [4]. The plasmid pOS8, which expresses β-galactosidase, was used as the control plasmid [19]. Each plasmid (1 μg/mL) was transfected into Huh 7.5.1, JFH1, and H77s at 50% confluence in 6-well plates using Lipofectamine 2000 (Life Technologies).

RNA Extraction, cDNA Synthesis and Real-time RT-PCR

Total RNA was extracted with TRIzol reagent (Life Technologies). Reverse transcription was carried out using the RT-PCR kit (Applied Biosystems, Foster City, CA, USA), and cDNA was quantified by real-time PCR using LightCycler technology and SYBR green I dye (Roche Diagnostics, Mannheim, Germany). Real-time PCR for PKR was performed with 2 μl of purified cDNA in a reaction SYBR green mixture containing 4 mM $MgCl_2$, and 5 pM each of forward primer (5′-AGCA-CACTCGCTTCTGAATC-3′) and reverse primer (5′-CTGGTCTCAGGATCATAATC-3′). PCR consisted of an initial denaturation step for 10 min at 95°C, then 40 cycles under the following conditions: 10 sec at 95°C, 10 sec at 58°C, and 15 sec at 72°C. For PCR amplification of GAPDH, c-Fos, c-Jun, and IL-8, commercial primer sets (Roche Search LC, Heidelberg, Germany) were used under conditions recommended by the

Table 1. Clinicopathological parameters of patients with hepatocellular carcinoma (HCC) (n = 34).

	Low PKR (n = 17)	High PKR (n = 17)	p-value
Age, years (range)	65 (36–82)	70 (49–79)	0.245
Gender (M/F)	14/3	13/4	1.000
Virus (HBV/HCV/None)	7/7/3	4/10/3	0.510
Child-Pugh (A/B/C)	15/2/0	17/0/0	0.145
Fibrosis (F1/F2/F3/F4)	2/3/3/9	2/3/3/9	1.000
Pathological stage (1/2/3/4)	6/6/3/1	2/9/6/0	0.206
AFP, ng/mL (range)	6.0 (1.6–1525)	25 (0–7720)	0.435
DCP, mAU/mL (range)	65 (13–418820)	212(16–45133)	0.356
PT, % (range)	86.9 (56–181)	85.10 (73–129)	0.790
Tumor size	24 (10–160)	35 (20–75)	0.816
Tumor differentiation (well/moderate/poor)	3/11/3	4/13/0	0.191
Tumor multiplicity (solitary/multiple)	13/4	13/4	1.000

HBV, hepatitis B virus; HCV, hepatitis C virus; AFP, alpha-fetoprotein; DCP, des-carboxyprothrombin; PT, prothrombin time.
doi:10.1371/journal.pone.0067750.t001

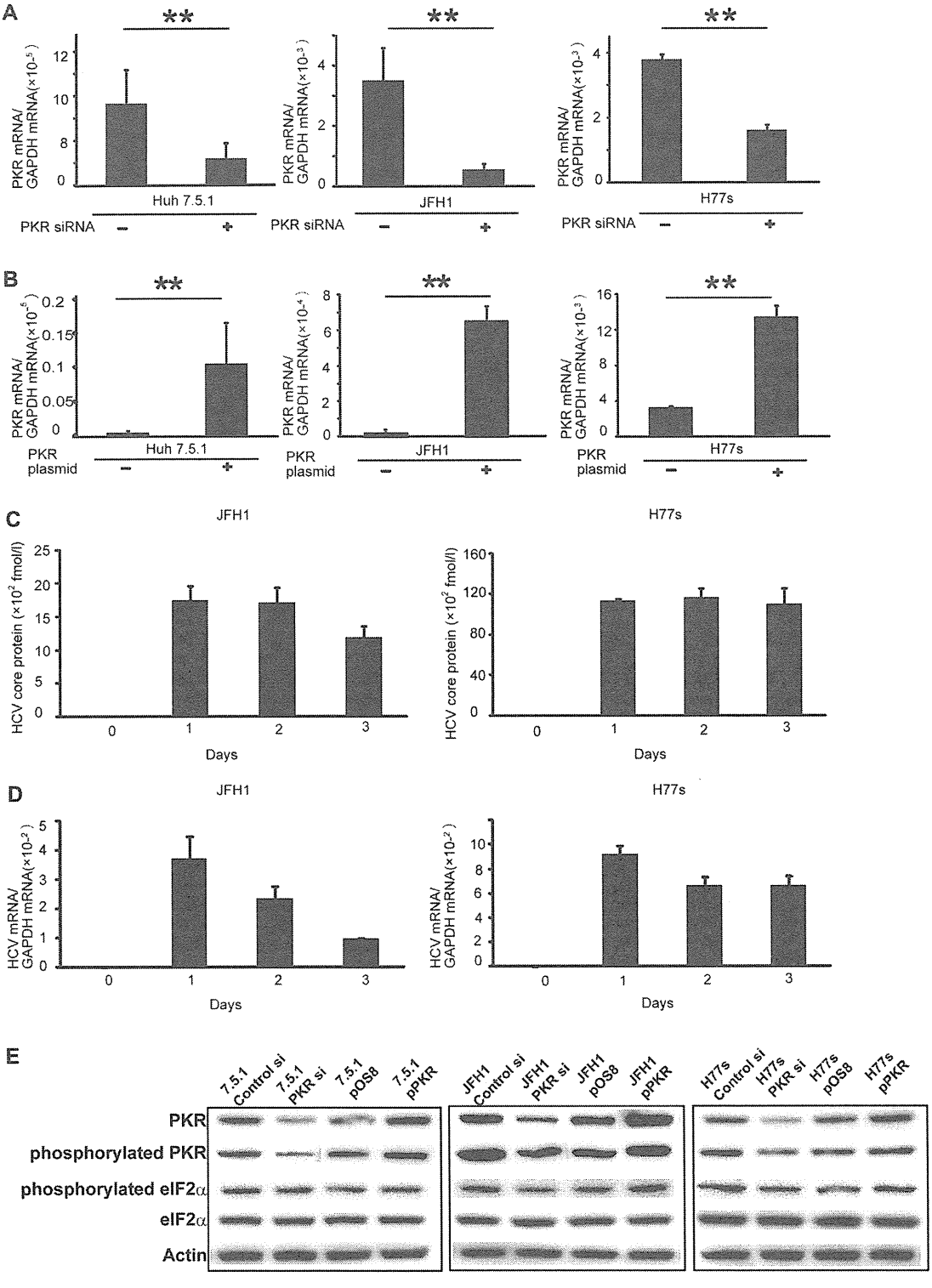

Figure 1. Down- and upregulation of PKR gene expression by PKR siRNA or by a PKR-expression plasmid, respectively, in liver cancer cell lines, Huh 7.5.1, JFH1 and H77s. Cells were transfected with either PKR siRNA or control siRNA, then PKR mRNA was quantified by real-time RT-PCR; PKR was knocked down (A). Cells were transfected with PKR-expression plasmid (pPKR) or control plasmid (pOS8), then subjected to real-time RT-PCR; PKR mRNA was upregulated by pPKR (B). Mean ± SEM of six replicates. **$p<0.01$. The amount of HCV core protein in JFH1 and H77s cells were measured by ELISA. HCV core protein was stably expressed in both cell types at least three days after transfection with the HCV-RNA

(C). The amount of HCV mRNA in JFH1 and H77s cells was measured by real-time RT-PCR. HCV RNA was expressed in both cell types at least three days after transfection with the HCV-RNA (D). Mean ± SEM of four replicates. PKR and phosphorylated PKR protein expression evaluated by Western blotting; results confirmed PKR mRNA data (E).
doi:10.1371/journal.pone.0067750.g001

manufacturer. PCR amplification of HCV RNA proceeded as described elsewhere [20]. The relative mRNA expression levels of target host genes were defined by dividing by the amount of GAPDH mRNA and were then evaluated by statistical analysis.

PCR Array Analysis

For comprehensive analysis of the role of PKR, the RT2 Profiler PCR array system (QIAGEN, Tokyo, Japan) and the LightCycler system (Roche) were used according to the manufacturers' instructions. Threshold cycle values were analyzed using web-based PCR array data analysis software found at http://www.sabiosciences.com/pcr/arrayanalysis.php. Of the kits supplied with the PCR array system, the Cancer PathwayFinder PCR array was used. Before applying the data, it was determined that the reverse transcriptase control, cDNA control, and positive PCR control levels were within the accepted range.

Western Blotting

Proteins were extracted with RIPA buffer comprising 10 mmol/L Tris, PH 7.4, 150 mmol/L NaCl, 0.5% v/v NP-40 and 1% w/v sodium dodecyl sulphate (SDS). For Western immunoblotting, 20 μg of protein were applied to lanes of 4–12% Bis-Tris Gels (Life Technologies), then blotted onto Immobilon-P membranes (Millipore, Bedford, MA, USA) and incubated with the relevant antibody: anti-beta-actin (Chemicon, Temecula, CA, USA), anti-PKR (product number: 3210), anti-eIF2α (5324), anti-phospho-eIF2α (3398), anti-Erk1/2 (4695), anti-phospho-Erk1/2 (4370), anti-JNK (9252), anti-phospho JNK (4668), anti-c-Jun (9165), anti-phosphor-c-Jun (3270), anti-c-Fos (2250) (Cell Signaling, Danvers, MA, USA), anti-phospho PKR (Life Technologies) or anti-phospho c-Fos (Abcam, Tokyo, Japan) antibody. Appropriate species-specific conjugated secondary antibody kits were commercially obtained (General Electric, Charles Coffin, NY, USA). Proteins were detected using the ECL Prime Kit or the ECL Kit (General Electric). Bands were quantified by normalization to β-actin using Image J Software (National Institutes of Health Bethesda, MD, USA).

Cell Proliferation Assay

Cell viability was quantified by a MTS assay (Promega, Fitchburg, WI, USA). After 24 h of siRNA or plasmid transfection in 6-well plates, cells were resuspended and then 2×10^3 cells were seeded in 96-well plates. At each time point, cells were treated with MTS reagent and incubated for 120 min. Absorbance at 450 nm was recorded. U0126 (Merck), a selective inhibitor of MAP kinase kinase (MEK), was used to inhibit the c-Fos signaling pathway, and SP600125 (Merck), a selective inhibitor of JNK, was used to inhibit the c-Jun signaling pathway.

Enzyme-linked Immunosorbent Assay for IL-8 and HCV Core Protein

Concentrations of IL-8 were measured in culture supernatant fluids using an enzyme-linked immunosorbent assay (ELISA) kit (R&D Systems, Minneapolis, MN, USA). The lower limit of detection for IL-8 was 31.2 pg/mL. HCV core antigen in cell lysates was quantified using HCV core antigen ELISA kits (Ortho-Clinical Diagnostics, Raritan, NJ, USA) following the manufacturer's instructions. The lower limit of detection for HCV was 44.4 fmol/L.

Luciferase Assays

Cells were transfected with a wild type IL-8 promoter conjugated to firefly luciferase reporter constructs (pIL-8) provided by Dr. Charalabos Pothoulakis (University of California, Los Angeles, CA, USA) [21], together with a control reporter plasmid conjugated with Renilla luciferase reporter constructs, phRL-TK^{Int-} (Promega). Luciferase activities in the samples were measured 48 h later using the Dual-Luciferase Reporter Assay System (Promega) and a luminometer (Microtec, Funabashi, Chiba, Japan). The level of transcription was evaluated as the ratio of firefly luciferase to Renilla luciferase.

Wound Healing Assay

JFH1 or H77s cells (2×10^5/well) were seeded into 6-well plates and incubated for two days. After confirming that a complete monolayer had formed, the monolayers were wounded by scratching lines onto the cultures using a plastic tip. The wells were then washed once to remove any debris, and observed and photographed under the microscope. Thereafter, the plates were incubated at 37°C in 5% CO2 for 48 h, after which the cells were observed and photographed. The distance that the cells had migrated was measured on the photomicrographs [22]. The percent wounded area filled was calculated as follows: {(mean wounded breadth − mean remaining breadth)/mean wounded breadth} ×100.

c-Fos and c-Jun Transcription Assay

The c-Jun and c-Fos transcription assay was performed using TransAM™ (Active Motif, Carlsbad, CA, USA) according to the manufacturer's instructions, to detect the DNA binding capacity of c-Jun or c-Fos containing AP-1 dimers. This assay is equivalent to the Electrophoresis Mobility Shift Assay (EMSA) used to evaluate DNA binding capacity [23]. Briefly, JFH1 cells were treated with PKR siRNA or control siRNA, and after 48 h, 10 μg of nuclear extract (containing activated transcription factor) was added to oligonucleotide-coated wells (containing 5′-TGAGTCA-3′). After 20 min of incubation at room temperature with mild agitation, the plate was washed, and then incubated with 100 μL/well of diluted anti-c-Jun or anti-c-Fos antibody for 1 h. The plate was washed three times and 100 μl HRP-conjugated antibody was added for 1 h. Developing solution was added for 10 min. The reaction was stopped and absorbance at 450 nm was determined.

Statistical Analysis

All statistical analyses were performed using SPSS 14.0 software (SPSS, Chicago, IL, USA). Data are expressed as mean ± SEM. Statistical differences were determined using the Mann-Whitney U test. The relationships between c-Fos and c-Jun were expressed as Pearson product-moment correlation coefficients. P-values < 0.05 were considered to be significant.

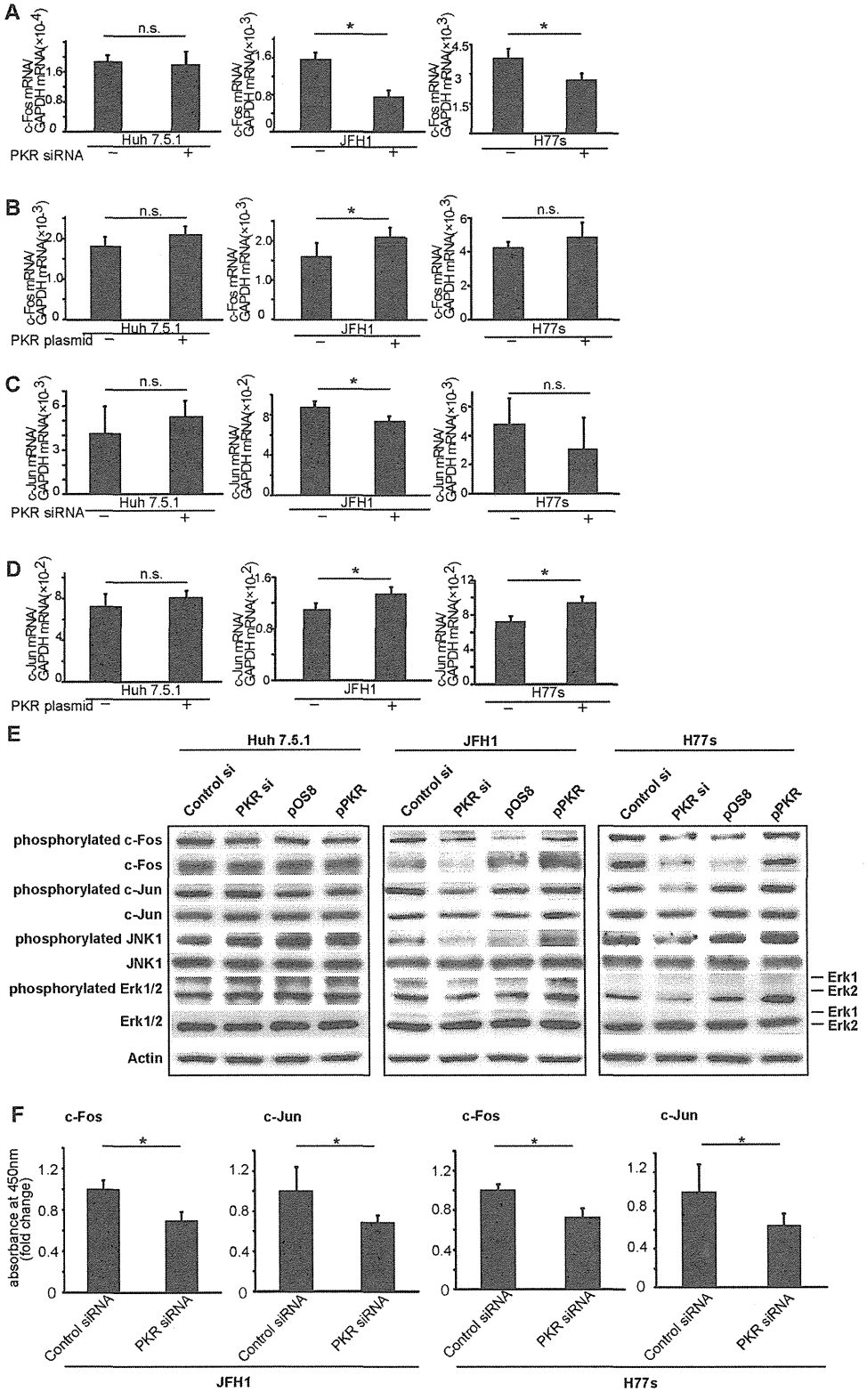

Figure 2. PKR upregulates c-Fos and c-Jun mRNA and protein in the HCC cell lines with HCV infection, JFH1 and H77s. Cells were transfected with either control or PKR siRNA, and with either control or PKR-expression plasmid (pPKR). c-Fos mRNA was decreased by PKR

knockdown (A), and c-Fos was upregulated by PKR overexpression (B). c-Jun mRNA was downregulated by PKR siRNA (C), and upregulated by pPKR (D). Mean ± SEM of six replicates. *p<0.05. n.s.: not significant. Protein expression of c-Fos, c-Jun, JNK1, Erk and their phosphorylated forms determined by Western blotting. Bothc-Fos and c-Jun signaling pathways were activated by PKR (E). DNA binding activities of c-Jun and c-Fos were downregulated by PKR knockdown (F). Mean ± SEM of six replicates. *p<0.05.
doi:10.1371/journal.pone.0067750.g002

Results

PKR Knockdown and Upregulation by PKR siRNA and PKR-encoding Plasmid in HCV-infected HCC Cells

PKR siRNA was designed to knock down PKR gene expression in liver cancer cell lines [18]. As shown by real-time RT-PCR, PKR siRNA efficiently knocked down PKR mRNA levels in Huh7.5.1, JFH1 and H77s cell lines by day 2 after transfection (Fig. 1A). Use of this method also revealed that the PKR-encoding plasmid (pPKR) efficiently upregulated PKR mRNA in experimental cell lines by day 2 after transfection (Fig. 1B).

The amount of HCV core protein was measured before (day 0) and after (days 1–3) transfection with HCV-RNA from pJFH1-full or pH77s-full. The HCV core protein expressed stably at least three days after the transfection in both JFH1 and H77s cells (Fig. 1C). The amount of HCV-RNA was also evaluated by real-time RT-PCR at the time core protein was measured in JFH1 and H77s cells (Fig. 1D). The level of HCV-RNA in JFH1 cells on day 3 was decreased, which may reflect the near-confluent cell culture condition, as reported previously [15]. However, HCV-RNA was expressed in both cell types at least three days after transfection.

Confirming results reported previously [7], HCV infection enhanced PKR activation, indicating upregulation of phosphorylated PKR, as shown in Fig. S1. Western blotting demonstrated the expected corresponding changes in PKR and phosphorylated PKR protein expression (Fig. 1E). To evaluate the influence of PKR activation, the expression of phosphorylated eIF2α was also determined. In the HCV-infected cells (JFH1 and H77s), the expression of phosphorylated eIF2α was altered by the knockdown or overexpression of PKR; however, in uninfected Huh 7.5.1 cells, the expression of phosphorylated eIF2α was not significantly altered (Fig. 1E). The expression of PKR, phosphorylated PKR, and phospohorylated eIF2α was quantified by normalizing to expression of β-actin using Image J Software (Fig. S2).

PKR Upregulates the AP-1 Family Transcription Factors c-Fos and c-Jun in HCV-infected HCC Cells

Use of the Cancer Pathway Finder PCR array indicated that several cancer pathways were modulated by up- or downregulation of PKR (Table S1). AP-1 family transcription factors, including c-Fos and c-Jun, were modulated in JFH1 cells, and the modulation was more evident in JFH1 than in uninfected Huh7.5.1 cells. Additionally, the interleukin IL-8 gene, which is a downstream AP-1 entity, was also altered by the PKR in JFH1 cells. These results indicated that the modulation of c-Fos and c-Jun by PKR was more evident because the function of PKR was enhanced by HCV infection. Real-time RT-PCR analysis of JFH1 confirmed modulation of c-Fos and c-Jun genes due to the expression of PKR with knockdown by PKR siRNA and with overexpression by PKR plasmid (Fig. 2A–D). Similar trends were observed in H77s, although some results were not statistically significant (Fig. 2A–D).

Alteration of the MAPK pathways, including of c-Fos and c-Jun, by PKR in the HCV-infected HCC cells became the next focus of investigation. Using Western blot analysis, the effect of modulation of PKR expression on expression of c-Fos and c-Jun protein was determined. When expression of PKR was knocked down by PKR siRNA, c-Fos and c-Jun expression were downregulated in JFH1 and H77s cells. Moreover, expression of both phosphorylated c-Fos and phosphorylated c-Jun correlated with the expression of PKR in JFH1 and H77s cells (Fig. 2E). Protein levels were quantified by normalizing to β-actin using Image J Software (Fig. S3).

Mediators upstream of c-Fos and c-Jun in the MAPK signaling pathway were assessed, and phosphorylated Erk1/2 (upstream of c-Fos) and phosphorylated JNK1 (upstream of c-Jun) were also found to positively correlate with expression of PKR (Fig. 2E), although the total expression levels of Erk1/2 and JNK1 were not changed. These results indicate that the PKR in HCC with HCV infection upregulates both the Erk1/2 to c-Fos and JNK1 to c-Jun signaling pathways. These alterations of MAPK pathways by PKR were not seen in Huh7.5.1 cells without HCV infection (Fig. 2E).

Additional confirmation that PKR positively regulates c-Fos and c-Jun signaling pathways was provided by use of the Trans AM™ Transcription Factor Assay Kit (Active Motif), which allows assessment of the DNA-binding capacity of c-Fos and c-Jun in a manner similar to the electrophoretic mobility shift assay (EMSA). Downregulation of PKR resulted in decreased DNA-binding capacity of c-Fos and c-Jun (Fig. 2F). Moreover, after the treatment by a PKR inhibitor, the expression of phosphorylated PKR was decreased, as shown by Western blotting analysis (Fig. S4). In addition, the expression of phosphorylated c-Fos and phosphorylated c-Jun was obviously decreased (Fig. S4). According to these results, we suggest that PKR would increase the phosphorylation of c-Fos and c-Jun, and then activate c-Fos and c-Jun directly.

PKR Induces Proliferation in HCC Cells with HCV Infection that Depends on Expression of c-Fos and c-Jun

It is well known that the MAPK pathway is associated with cell proliferation [24,25]. Therefore, assessments of proliferation were performed. Monolayer wound healing experiments revealed that JFH1 and H77s cells recovered more slowly after PKR knockdown than after transfection with control siRNA (Fig. 3A, B).

Additionally, effects on cell proliferation were evaluated by the MTS assay. Cell proliferation decreased significantly after PKR knockdown by PKR siRNA, and increased significantly when PKR was upregulated by pPKR in the JFH1 and H77s cells ($p<0.01$) (Fig. 3C). However these alterations of cell proliferation were not evident in Huh7.5.1 cells without HCV infection (Fig. S5).

To determine which signaling pathways are operational in cell proliferation induced by PKR, inhibition assays, using U0126 to inhibit the c-Fos pathway and SP600125 to inhibit the c-Jun pathway, were performed. We confirmed the effects of these compounds against c-Fos and c-Jun. The expression of phosphorylated c-Fos or phosphorylated c-Jun was evaluated by Western blotting after 24 h incubation with U0126 or SP600125 in both JFH1 and H77s cells (Fig. S6). The U0126 decreased phosphorylated c-Fos, but the effect on phosphorylated c-Jun was not evident in either JFH1 or H77s. SP600125 decreased phosphorylated c-Jun, but the effect on phosphorylated c-Fos was not evident. JFH1 proliferation was increased after the upregulation of PKR, and this increase was significantly diminished by either U0126 or SP600125 ($p<0.05$) (Fig. 3D). Use of both U0126 and SP600125 further diminished proliferation ($p<0.05$) to a level

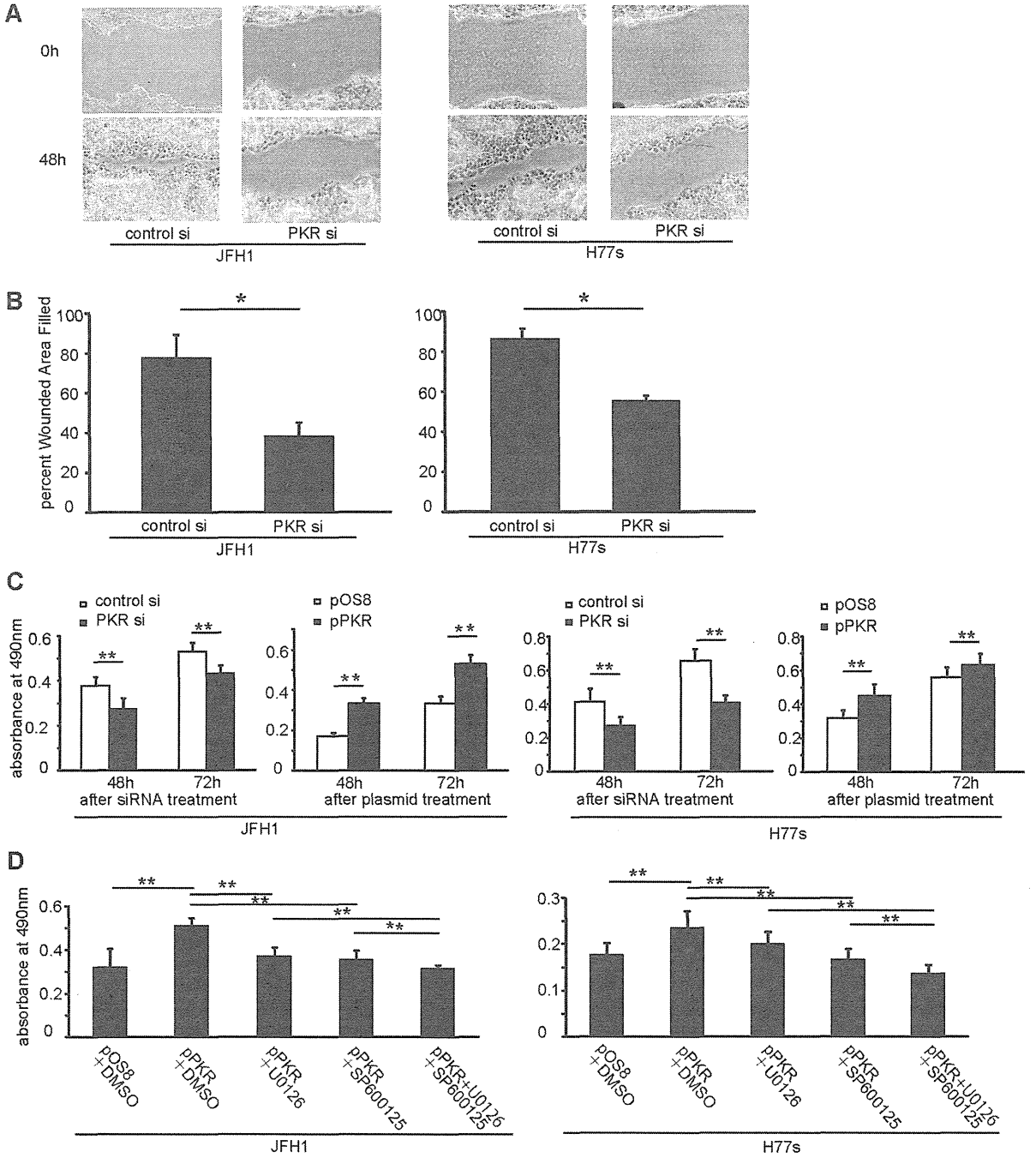

Figure 3. PKR expression was associated with proliferation of JFH1 and H77s cells, which was dependent on both c-Fos and c-Jun signaling pathways. Wound healing assay: Confluent monolayers of JFH1 or H77s cells transfected with PKR siRNA or control siRNA were wounded by scratching, and incubated for 48 h (A). Percent wounded area filled in with JFH1 and H77s cells (B). Mean ± SEM of six replicates. MTS assay: Proliferation was associated with PKR expression (C). Cells were transfected with pPKR, and then 20 μM c-Jun inhibitor (SP600125) and 10 μM c-Fos inhibitor (U0126) was added. MTS assay indicated that cell proliferation induced by PKR depended on both c-Jun and c-Fos pathways (D). Mean ± SEM of 10 replicates. **p<0.01, *p<0.05.
doi:10.1371/journal.pone.0067750.g003

similar to that of JFH1 cells transfected with control plasmid (pOS8). These results indicate that both c-Fos and c-Jun signaling pathways mediate PKR-induced cell proliferation in these HCV-infected HCC cell lines.

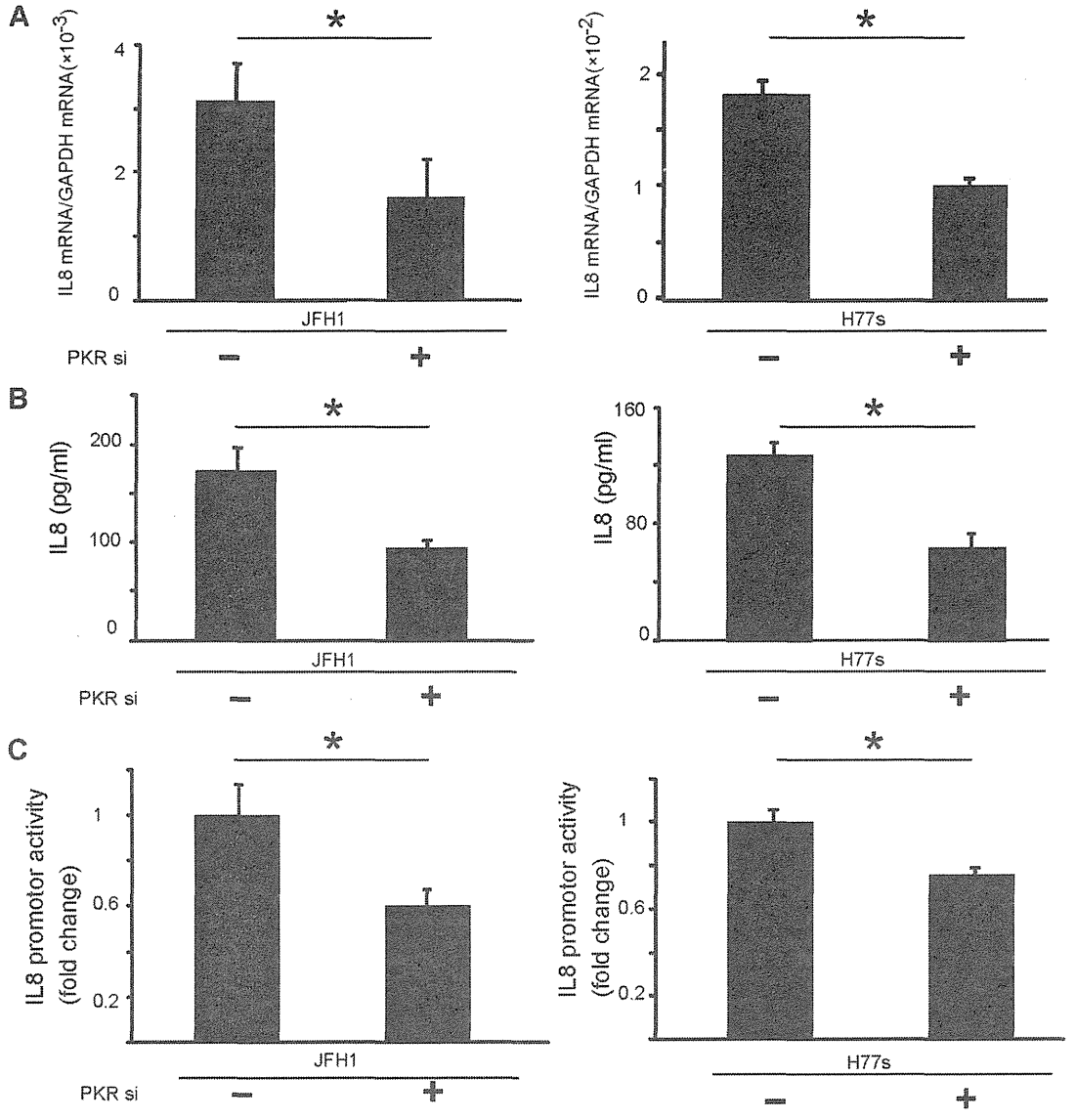

Figure 4. The PKR upregulates IL-8 expression and secretion. IL8 mRNA levels were downregulated by PKR knockdown (A). Supernatants of cultured cells were collected, and IL-8 levels were determined by ELISA. Secreted IL-8 was downregulated by PKR knock-down (B). Assays using the IL-8 promoter-luciferase reporter plasmid: IL-8 promoter activities were downregulated by PKR knockdown (C). Mean ± SEM of six replicates. *$p<0.05$.
doi:10.1371/journal.pone.0067750.g004

PKR Positively Regulates IL-8 Expression

RT-PCR revealed that IL-8 mRNA was downregulated significantly by PKR knockdown ($p<0.05$) (Fig. 4A), as were levels of secreted IL-8 protein in culture supernatants (Fig. 4B). IL-8 promoter activity also decreased after PKR knockdown (Fig. 4C). Thus, PKR-modulated c-Jun and c-Fos influenced production of IL-8, a molecule downstream of c-Jun and c-Fos signaling.

c-Jun and c-Fos were Activated by PKR Expression in Human HCC Tissue with HCV Infection

The mRNA levels of c-Fos and c-Jun in 34 specimens of human HCC tissues were determined. The specimens were divided by median PKR mRNA level into two groups of higher (High PKR) and lower (Low PKR) levels. Median values for PKR mRNA in all HCC specimens, in HCC specimens with HCV infection, and in HCV-unrelated HCC specimens were 1.00×10^{-3}, 1.20×10^{-3}, and 8.00×10^{-4} copy ratio (PKR mRNA/GAPDH mRNA), respectively.

When considering all 34 HCC specimens together, the High PKR Group had significantly higher levels of c-Jun mRNA than did the Low PKR group ($p = 0.024$). For HCC specimens with HCV infection, the c-Jun mRNA level of the High PKR group was significantly higher than that of the Low group ($p = 0.021$), but this difference was not evident in the HCC specimens without HCV infection (Fig. 5A). The levels of c-Fos mRNA did not differ significantly among these groups (Fig. 5B). However, a positive

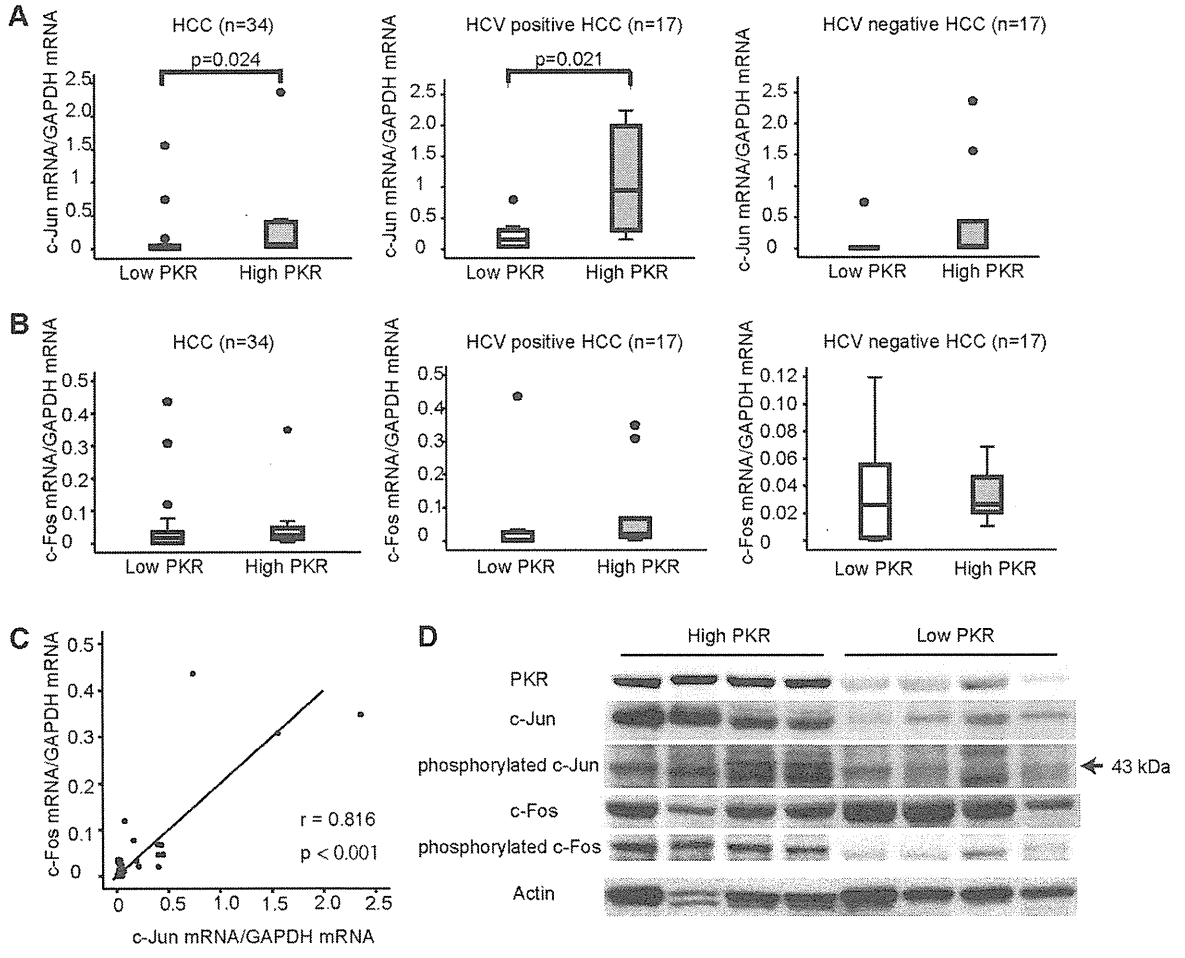

Figure 5. c-Jun and c-Fos were activated by the expression of PKR in human HCC tissues with HCV infection. RNA from HCC specimens of 34 patients, 17 HCC specimens with HCV infection (HCC positive HCC), and 17 HCC without HCV infection (HCC negative HCC). Each group was divided into two subsections by the median PKR mRNA values: Low PKR and High PKR. c-Jun mRNA (A) and c-Fos mRNA (B) were measured. c-Fos mRNA significantly correlated with c-Jun mRNA ($r = 0.816$, $P < 0.001$) (C). The four human HCC specimens having the highest (High PKR) and the four having the lowest (Low PKR) PKR protein expression were analyzed by Western blotting. c-Jun and c-Fos in the High PKR group were activated more than in the Low PKR group (D).
doi:10.1371/journal.pone.0067750.g005

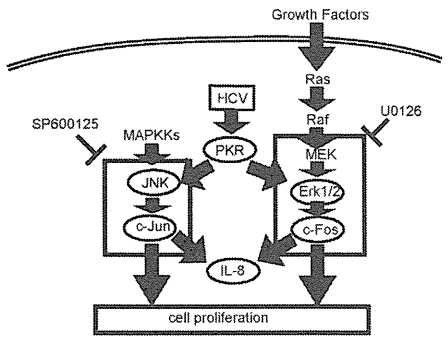

Figure 6. Model of the role of PKR in cell proliferation and relationships between PKR and other molecules associated with the c-Jun and c-Fos pathways. SP600125: inhibitor of c-Jun pathway. U0126: inhibitor of c-Fos pathway.
doi:10.1371/journal.pone.0067750.g006

correlation between c-Fos and c-Jun mRNA levels was observed ($r = 0.816$, $P < 0.001$) (Fig. 5C).

Additional Western blotting was performed to evaluate phosphorylated c-Jun and c-Fos levels in the human HCC specimens. The four specimens having the highest and the four having the lowest expression of PKR proteins were assayed. The specimens from the High PKR group had greater expression of phosphorylated c-Jun and phosphorylated c-Fos (Fig. 5D). These results indicate that PKR expression is related to activation of c-Jun and c-Fos in the human HCC specimens used in this study.

Discussion

Protein kinase R (PKR) is well known as a key molecule in elimination of HCV, especially during interferon use [18]. A previously reported study demonstrated that PKR is overexpressed in HCC tissues; however, its precise role in HCC-related phenomena remains controversial. It was reported that PKR plays a tumor suppressor function through the p53 signaling

pathway in human colon cancer cell lines [26]. However, other recent reports indicate that PKR can directly stimulate cell growth through the p38 MAPK and NF-κB pathways [27,28]. The p38MAPK pathway is known to play a critical role in the pathogenesis of various malignancies [29,30], and NF-κB is known to regulate inflammatory cytokines, growth factors, angiogenic factors and anti-apoptotic effects, each of which can contribute to the process of carcinogenesis [31]. Initially, the focus of the current study was on those molecules; however, the p53, p38MAPK and NF-κB pathways were not altered by PKR expression in the HCC cell lines with HCV infection that were used (Table S1). Moreover, results from examination of the cell cycle by FACS analysis and staining with propidium iodide revealed that the proportion of the sub-G1 population was not altered by the downregulation or upregulation of PKR (data not shown). It is possible that the role of PKR in HCC with HCV infection has a specialized function because PKR is directly induced and activated by HCV; otherwise, levels of activated PKR would be higher in this setting than in other cancers.

This study demonstrated that PKR is more highly activated in HCC cells with HCV infection, and that under those conditions, the over-activated PKR upregulates c-Jun and c-Fos through activation of JNK1 and p44/42 MAPK (Erk1/2), respectively (Fig. 6). Upregulation of c-Jun and c-Fos was dependent on tumor cell proliferation, and in turn induced IL-8. Activation of c-Jun and c-Fos was also observed in the human HCC specimens, in which PKR was overexpressed. The functions of over-activated PKR would be expected to have negative effects on prognosis for HCC patients with HCV infection, and could be related to the worse outcomes observed in this setting.

c-Jun and c-Fos are members of the activating protein 1 (AP-1) family. These proteins are diametric transcription factors [32] that bind to DNA [33]. The AP-1 family is implicated in carcinogenesis, and it regulates genes that include important regulators of invasion and metastasis, proliferation, differentiation, and survival [34]. Among the AP-1 proteins, c-Jun is able to both homo- and heterodimerize, whereas c-Fos is unable to homodimerize. In vitro studies have shown that Jun-Fos heterodimers are more stable and have stronger DNA-binding activity than Jun-Jun homodimers [35]. The current results in human HCC tissues indicated a positive correlation between levels of c-Fos and c-Jun (Figure 6C), suggesting that c-Jun and c-Fos hetero-dimers could be the main moieties binding to DNA in HCC.

Previous reports indicated that c-Jun is important for hepatogenesis [36,37]. In mice with inactivated c-Jun, the number and size of hepatic tumors caused by diethylnitrosamine (DEN) treatment were reduced [38], suggesting that c-Jun may have an important role in tumor progression. On the other hand, persistent expression of c-Fos would also play an important role in tumor progression. c-Fos is known to induce depolarization and acquisition of an invasive phenotype, a process generally referred to as "epithelial to mesenchymal transition" (EMT) [39], resulting in tumor growth and metastasis. In a previous study of 150 human HCC samples, c-Fos expression was significantly higher in tumors than in non-tumor tissue ($p<0.0001$) [40], and elevated JNK1 (the c-Jun upstream activator) activity was identified in more than 50% of HCC samples relative to non-cancerous liver tissue [41]. In the current study, upregulation of c-Jun was identified in HCC tissues with higher expression of PKR. These findings suggest that alterations of c-Jun and c-Fos pathways in HCC with HCV infection may have important roles in tumor progression.

The direct effects of HCV on the c-Jun and c-Fos pathways must be considered. A previous report suggests that HCV proteins can modulate MAPK (Erk) signaling by targeting multiple steps along the signaling pathways [42]. Another report indicated that HCV E2 protein activates the MAPK (Erk) pathway and promotes cell proliferation in human hepatoma Huh-7 cells [42]. The current results suggest that PKR may activate Erk1/2 directly through phosphorylation. The previous reports did not describe PKR expression, and it is possible HCV proteins modulate the MAPK (Erk) pathway through the activation of PKR. On the other hand, one previous report described negative regulation of Erk by PKR, but positive regulation of JNK by PKR in mouse embryonic stem cells [43]. HCV infection may alter the role of PKR with respect to the c-Jun and c-Fos pathways: differences in this role in HCC as compared to other cancer types need to be determined in future studies. Recently, the multikinase inhibitor, sorafenib, was reported to be effective for treatment of HCC [44]. Sorafenib was shown to inhibit c-Raf, Erk and MAPK/Erk kinase (MEK) [44], and therefore would have a greater effect in HCC patients with HCV. The role of PKR in treatment with sorafenib should be addressed in future analyses.

Over-activated PKR in HCC with HCV infection upregulated production of IL-8 in this study. IL-8 occurs downstream to AP-1 [45], and is known to contribute to angiogenesis and proliferation [46] in various cancers. It is known that HCV NS5A can induce IL-8 mRNA and protein [47], and in a previous report, serum levels of IL-8 were increased significantly in patients with chronic hepatitis C compared with normal controls [48]. Activated PKR could contribute to the upregulation of IL-8 in patients with HCV, which could in turn contribute to tumor progression. The precise role of upregulated IL-8 in HCC with HCV infection also needs to be ascertained in detail in future studies.

In conclusion, the current results demonstrate that over-activated PKR in HCC with HCV infection contributes to proliferation due to the upregulation of c-Jun and c-Fos by activation of JNK and Erk1/2. Such effects of over-activated PKR would be expected to have negative effects on treatment of HCC patients with HCV infection. The role of PKR and its importance for elimination of HCV in patients with HCC needs to be reconsidered. Over-activated PKR potentially could serve as a therapeutic target in HCC patients with HCV infection; further studies are warranted to investigate this possibility.

Supporting Information

Figure S1 HCV infection upregulates the expression of phosphorylated PKR protein. 24 h after transfection of Huh 7.5.1cells with pJFH1-full or pH77s-full, protein expression of PKR and phosphorylated PKR were determined by Western blotting. In the HCV-infected HCC cells (JFH1 and H77s), expression of phosphorylated PKR was increased significantly compared with that in Huh7.5.1 cells (HCV-uninfected HCC cells).
(TIF)

Figure S2 Quantification of Figure 1E Western blot bands. Bands in Figure 1E indicating PKR, phosphorylated PKR and phosphorylated eIF2α were quantified and normalized using the quantified corresponding beta-actin band.
(TIF)

Figure S3 Quantification of Figure 2E Western blot bands. Bands in Figure 2E indicating c-Fos, c-Jun, phosphorylated c-Fos and phosphorylated c-Jun were quantified and normalized using the quantified corresponding beta-actin band.
(TIF)

Figure S4 PKR inhibitor decreased phosphorylation of c-Fos and c-Jun. PKR inhibitor (300 nM) was added to JFH1

and H77s. After a 24 h treatment, the expression of PKR, c-Fos, c-Jun, phosphorylated PKR, phosphorylated c-Fos, and phosphorylated c-Jun were evaluated by Western blotting. PKR inhibitor decreased phosphorylated PKR, and phosphorylated c-Jun and phosphorylated c-Fos proteins.
(TIF)

Figure S5 Enhancement of cell proliferation was not evident in Huh7.5.1 cells without HCV infection. Wound healing assay: Confluent monolayers of Huh7.5.1 cells transfected with PKR siRNA or control siRNA were wounded by scratching and then incubated for 48 h (A). Percent wounded area filled in with Huh7.5.1 cells. Mean ± SEM of six replicates (B). MTS assay: Proliferation was not associated with PKR expression in Huh7.5.1 (C). Mean ± SEM of 10 replicates.
(TIF)

Figure S6 U0126 inhibits c-Fos signaling pathway, and SP600125 inhibits c-Jun signaling pathway, in JFH1 and in H77s cells. 10 μM c-Fos inhibitor (U0126) or 20 μM c-Jun inhibitor (SP600125) was added to JFH1 and H77s cell cultures. After a 24 h treatment, levels of phosphorylated c-Fos and phosphorylated c-Jun were evaluated by Western blotting. U0126 decreased phosphorylated c-Fos, and SP600125 decreased phosphorylated c-Jun.
(TIF)

Table S1 PCR array analysis of the effect of PKR up- and down-regulation on cancer-related genes.
(DOC)

Acknowledgments

We thank the following individuals: Dr. Takaji Wakita, Department of Virology II, National Institute of Infectious Diseases, Tokyo, Japan, for providing JFH-1; Dr. Stanley M. Lemon, Division of Infectious Diseases, University of North Carolina at Chapel Hill, Chapel Hill, NC, USA and Dr. Francis V. Chisari, Department of Immunology and Microbial Science, The Scripps Research Institute, La Jolla, CA, USA, for providing Huh7.5.1 cells; Dr. Michael Gale, Jr., Department of Immunology, University of Washington, Seattle, WA, USA, for providing plasmid PKR; and Dr. Charalabos Pothoulakis, Division of Digestive Diseases, University of Califonia, Los Angeles, CA, USA, for providing luciferase reporter constructs for IL-8. We thank Ms. Satomi Yamanaka, Ms. Sakiko Inoh, Ms. Chie Takeichi and Mr. Kenji Tanimoto for their valuable technical assistance.

Author Contributions

Conceived and designed the experiments: TW YH MO. Performed the experiments: TW YH YT. Analyzed the data: TW YH. Contributed reagents/materials/analysis tools: TW YH YT MH. Wrote the paper: TW YH RTC. Manuscript editing: TW YH YT MH MA YI BM RTC MO.

References

1. Alter MJH (1997) Epidemiology of hepatitis C. Hepatology 26: 62–65.
2. Okuda K (1998) Hepatitis C and hepatocellular carcinoma. J Gastroenterol Hepatol 13: 294–298.
3. Clemens MJ, Elica A (1997) The double-stranded RNA-dependent protein kinase PKR: Structure and function. J Interferon Cytokine Res 17: 503–524.
4. Meurs EF, Galabru J, Barber GN, Katze MG, Hovanessian AG (1993) Tumor suppressor function of the interferon-induced double stranded RNA-activated protein kinase. Proc Natl Acad Sci USA 90: 232–236.
5. Samuel CE (1979) Mechanism of interferon action: Phosphorylation of protein synthesis initiation factor eIF-2 in interferon-treated human cells by a ribosome-associated kinase processing site specificity similar to hemin-regulated rabbit reticulocyte kinase. Proc Natl Acad Sci USA 76: 600–604.
6. Gale M Jr., Tan SL, Katze MG (2000) Translational control of viral gene expression in eukaryotes. Microbiol Mol Biol Rev 64: 239–280.
7. Pflugheber J, Fredericksen B, Sumpter R Jr., Wang C, Ware F, et al. (2002) Regulation of PKR and IRF-1 during hepatitis C virus RNA replication. Proc Natl Acad Sci USA 99: 4650–4655.
8. Rivas-Estilla AM, Svitkin Y, Lastra ML, Hatzoglou M, Sherker A, et al. (2002) PKR-dependent mechanism of gene expression from a subgenomic hepatitis C virus clone. J Virol 76: 10637–10653.
9. Chang KS, Cai Z, Zhang C, Sen GC, Williams BR, et al. (2006) Replication of hepatitis C virus (HCV) RNA in mouse embryonic fibroblast: Protein kinase R (PKR)-dependent and PKR-independent mechanisms for controlling HCV RNA replication and mediating interferon activities. J Virol 80: 7364–7374.
10. Hiasa Y, Kamegaya Y, Nuriya H, Onji M, Kohara M, et al. (2003) Protein kinase R is increased and is functional in hepatitis C virus-related hepatocellular carcinoma. Am J Gastroenterol 98: 2528–2534.
11. Proud CG (1995) PKR: A new name and new roles. Trends Biochem Sci 20: 241–246.
12. Wiliams BRG (1995) The role of the dsRNA-activated kinase, PKR, in signal transduction. Semin Virol 6: 191–202.
13. Donze O, Jagus R, Koromilas AE, Hershey JW, Sonenberg N (1995) Abrogation of translation initiation factor eIF-2 phosphorylation causes malignant transformation of NIH 3T3 cells. EMBO J 14: 3828–3834.
14. Koromilas AE, Roy S, Barber GN, Katze MG, Sonenberg N (1992) Malignant transformation by a mutant of the IFN-inducible dsRNA-dependent protein kinase. Science 257: 1685–1689.
15. Wakita T, Pietschmann T, Kato T, Date T, Miyamoto M, et al. (2005) Production of infectious hepatitis C virus in tissue culture from a cloned viral genome. Nat Med 11: 791–796.
16. Yi MK, Lemon SM (2004) Adaptive Mutations Producing Efficient Replication of Genotype 1a Hepatitis C Virus RNA in Normal Huh7 Cells. J Virol 78: 7904–7915.
17. Yi MK, Villanueva RA, Thomas DL, Wakita T, Lemon SM (2006) Production of infectious genotype 1a hepatitis C virus (Hutchinson strain) in cultured human hepatoma cells. Proc Natl Acad Sci USA 103: 2310–2315.
18. Tokumoto Y, Hiasa Y, Horiike N, Michitaka K, Matsuura B, et al. (2007) Hepatitis C virus expression and interferon antiviral action is dependent on PKR expression. J Med Virol 79: 1120–1127.
19. Chung RT, He W, Saquib A, Conteras AM, Xavier RJ, et al. (2001) Hepatitis C virus replication is directly inhibited by IFN-alpha in a full-length binary expression system. Proc Natl Acad Sci USA 98: 9847–9852.
20. Hiasa Y, Kuzuhara H, Tokumoto Y, Konishi I, Yamashita N, et al. (2008) Hepatitis C virus replication is inhibited by 22beta-methoxyolean-12ene-3beta, 24(4beta)-diol (ME3738) through enhancing interferonbeta. Hepatology 48: 59–69.
21. Zhao D, Keates AC, Kuhnt-Moore S, Moyer MP, Kelly CP, et al. (2001) Signal transduction pathways mediating neurotensin-stimulated interleukin-8 expression in human colonocytes. J Biol Chem 276: 44464–44471.
22. Ohta H, Hamada J, Tada M, Aoyama T, Furuuchi K, et al. (2006) HOXD3-overexpression increases integrin αvβ3 expression and deprives E-cadherin while it enhances cell motility in A549 cells. Clin Exp Metastasis 23: 381–390.
23. Renard P, Ernest I, Houbion A, Art M, Le Calvez H, et al. (2001) Development of a sensitive multi-well colorimetric assay for active NFkappaB. Nucleic Acids Res 29: e21.
24. Gollob JA, Wilhelm S, Carter C, Kalley SL (2006) Role of Raf kinase in cancer: therapeutic potential of targeting the Raf/MEK/ERK signal transduction pathway. Semin Oncol 33: 392–406.
25. Nishina H, Wada T, Katada T (2004) Physiological Roles of SAPK/JNK Signaling Pathway. J Biochem 136: 123–126.
26. Yoon CH, Lee ES, Lim DS, Bae YS (2009) PKR, a p53 target gene, plays a crucial role in the tumor-suppressor function of p53. Proc Natl Acad Sci USA 106: 7852–7857.
27. Gou KC, de Veer MJ, Williams BR (2000) The protein kinase PKR is required for p38 MAPK activation and the innate immune response for p38 MAPK activation and the innate immune response to bacterial endotoxin. EMBO J 19: 4292–4297.
28. Dev A, Haque SJ, Mogensen T, Silverman RH, Williams BR (2001) RNA-dependent protein kinase PKR is required for activation of NF-κB by IFN-γ in a STAT1-independent pathway. J Immunol 166: 6170–6180.
29. Schultz RM (2003) Potential of p38 MAP kinase inhibitors in the treatment of cancer. Prog Drug Res 60: 59–92.
30. Hideshima T, Akiyama M, Hayashi T, Richardson P, Schlossman R, et al. (2003) Targeting p38 MAPK inhibits multiple myeloma cell growth in the bone marrow milieu. Blood 101: 703–705.
31. Maeda S, Omata M (2008) Inflammation and cancer: Role of nuclear factor-kappaB activation. Cancer Sci 99: 836–842.
32. Shaulian E (2010) AP-1-The Jun proteins: Oncogenes or tumor suppressors in disguise? Cell Signal 22: 894–899.
33. Lamph WW, Wamsley P, Sassone-Corsi P, Verma IM (1988) Induction of proto-oncogene JUN/AP-1 by serum and TPA. Nature 334: 629–631.
34. Milde-Langosch K (2005) The Fos family of transcription factors and their role in tumorigenesis. Eur J Cancer 41: 2449–2461.

35. Ryseck RP, Bravo R (1991) c-Jun, JunB, and JunD differ in their binding affinities to AP-1 and CRE consensus sequences: effect of fos protein. Oncogene 6: 533–542.
36. Eferl R, Sibilia M, Hilberg F, Fuchsbichler A, Kufferath I, et al. (1999) Functions of c-Jun in liver and heart development. J Cell Biol 145: 1049–1061.
37. Behrens A, Sibilia M, David JP, Mohle-Steinlein U, Tronche F, et al. (2002) Impaired postnatal hepatocyte proliferation and liver regeneration in mice lacking c-jun in the liver. EMBO J 21: 1782–1790.
38. Eferl R, Ricci R, Kenner L, Zenz R, David JP, et al. (2003) Liver tumor development. C-Jun antagonizes the proapototic activity of p53. Cell 112: 181–192.
39. Reichmann E, Schwarz H, Deiner EM, Leitner I, Eilers M, et al. (1992) Activation of an inducible c-FosER fusion protein causes loss of epithelial polarity and triggers epithelial-fibroblastoid cell conversion. Cell 71: 1103–1116.
40. Yuen MF, Wu PC, Lai VC, Lau JY, Lai CL (2001) Expression of c-Myc, c-Fos, and c-jun in hepatocellular carcinoma. Cancer 91: 106–112.
41. Chang Q, Zhang Y, Beezhold KJ, Bhatia D, Zhao H, et al. (2009) Sustained JNK1 activation is associated with altered histone H3 methylation in human liver cancer. J Hepatol 50: 323–333.
42. Zhao LJ, Wang L, Ren H, Cao J, Li L, et al. (2005) Hepatitis C virus E2 protein promotes human hepatoma cell proliferation through the MAPK/ERK signaling pathways via cellular receptors. Exp Cell Res 305: 23–32.
43. Takeda Y, Ichikawa H, Pataer A, Swisher S, Aggarwal BB (2007) Genetic deletion of PKR abrogates TNF-induced activation of IκBα kinase, JNK, Akt and cell proliferation but potentiates p44/p42 MAPK and p38 MAPK activation. Oncogene 26: 1201–1212.
44. Cheng AL, Kang YK, Chen Z (2009) Efficacy and safety of sorafenib in patients in the Asia-Pacific region with advanced hepatocellular carcinoma: a phase III randomised, double-blind, placebo-controlled trial. Lancet Oncol 10: 25–34.
45. Murayama T, Ohara Y, Obuchi M, Khabar KS, Higashi H, et al. (1997) Human cytomegalovirus induces interleukin-8 production by a human monocytic cell line, THP-1, through acting concurrently on AP-1- and NFκB-binding sites of the interleukin-8 gene. J Virol 71: 5692–5695.
46. Ning Y, Manegold PC, Hong YK, Zhang W, Pohl A, et al. (2011) Inteleukin-8 is associated with proliferation, migration, angiogenesis and chemosensitivity in vitro and in vivo in colon cancer cell line models. Int J Cancer 128: 2038–2049.
47. Polyak SJ, Khabar KSA, Paschal DM, Ezelle HJ, Duverlie G, et al. (2001) Hepatitis C Virus Nonstructural 5A protein induces Interleukin-8, leading to partial inhibition of the Interferon-induced antiviral response. J Virol 75: 6095–6106.
48. Masumoto T, Ohkubo K, Yamamoto K, Ninomiya T, Abe M, et al. (1998) Serum IL-8 levels and localization of IL-8 in liver from patients with chronic viral hepatitis. Hepato-Gastroenterology 45: 1630–1634.